A New Metastable Phase of Needle-like Nanocrystalline $VO_2 \cdot H_2O$ and Phase Transformation

Z. Gui,*,† R. Fan,*,† X. H. Chen,*,‡,1 and Y. C. Wu†

Structure Research Laboratory, †Department of Chemistry, and ‡Department of Physics, University of Science and Technology of China, Hefei, 230026, People's Republic of China

Needle-like nanocrystalline $VO_2 \cdot H_2O$, crystallized in a new metastable phase with orthorhombic symmetry ($a = 6.015$, $b = 4.642$, and $c = 3.763$ Å), was synthesized by a long hydrothermal reaction from NH_4VO_3 and hydrazine. The structure and composition of these nanocrystallites were characterized by X-ray powder diffraction, transmission electron microscopy, selected area electron diffraction, infrared absorbency spectroscopy, and thermogravimetric analysis. The influence of chemical reaction conditions on the features of the final products was investigated, and the optimum conditions were found to be 170°C for 15 days with a N_2H_4 concentration of 8.0%. Differential scanning calorimetry was conducted to study the phase transformation from as-prepared metastable $VO_2 \cdot H_2O$ to the more stable $(B)VO_2$ and rutile-type VO_2. © 2001 Academic Press

Key Words: novel phase; $VO_2 \cdot H_2O$; hydrothermal synthesis; phase transformation.

INTRODUCTION

The binary vanadium oxides, VO_x ($1 \leq x \leq 2.5$), exhibit a wide variety of structure types (1). Many of them are of technological importance with uses in oxidation catalysis (2), high-energy density battery electrodes (3), etc. These oxides also show interesting electronic properties, from metallic behavior in some VO_2 polymorphs to semiconducting behavior in V_2O_5. The rutile-tpye VO_2 displays a metal–insulator transition with increasing temperature (4, 5).

VO adopts a cubic rock salt structure, which contains a high percentage of defects. V_2O_3 adopts a structure similar to that of corundum (6). Monoclinic crystalline V_3O_5 was reported by Asbrink *et al.* (7). Vanadium also forms a number of binary oxides of the general formula V_nO_{2n-1} ($4 \leq n \leq 8$) and V_nO_{2n+1} ($n = 3, 4$, and 6) (8). The former are known as triclinic Magneli phases (9). The most oxygen-rich phase, V_2O_5, has been characterized with a layered

structure, which can be reduced by intercalation reactions to derive novel materials (10). Six phases of VO_2 are known; so far to our knowledge. Rutile-type VO_2, crystallized in the space group $P4/mmm$, is the thermodynamically most stable phase (11). Andersson discovered a monoclinic $P2_1/c$ phase of VO_2, (12) and a structurally similar triclinic VO_2 phase has also been identified (13). The three phases of VO_2 are interconverted in the temperature range from 325 to 340 K. A pioneering work on soft chemical routes to metastable phases of VO_2 or its hydrates was carried out by Theobald (14). $(A)VO_2$ was precipitated at a hydrothermal reaction temperature between 220°C and 330°C from a suspension of V_2O_3 and V_2O_5. Oka *et al.* determined its structure to be of tetragonal symmetry ($a = 11.90$ and $c = 7.68$ Å) (15). In this experiment, $(B)VO_2$ and rutile VO_2 were obtained below 220°C and above 330°C, respectively. $(B)VO_2$ also exists as an intermediate in the course of the thermal reduction of V_2O_5 by H_2 or SO_2 gas (16). It has a layered structure and shows good performance as an anode host for rechargeable lithium cell with aqueous electrolytes (17). Recently, Hagonman *et al.* prepared a new layered polymorph of VO_2 designated $(C)VO_2$ (18). Its hydrate $VO_2 \cdot 1/2H_2O$ has a structure analogous to that of recognized $Li_xV_{2-\delta}O_{4-\delta} \cdot H_2O$. Several intermediate metastable phases, such as $V_2O_5 \cdot H_2O$ and $V_3O_7 \cdot H_2O$, have been identified (19, 20).

Herein we report the synthesis of a novel metastable phase of $VO_2 \cdot H_2O$ by hydrothermal reaction of NH_4VO_3 and N_2H_4, which acts as a reducing agent and also could allow control of the size and morphology. The products obtained hydrothermally were comprised of phase-pure needle-like nanocrystallites. The phase transformation from as-prepared $VO_2 \cdot H_2O$ upon heating to 620°C has been investigated.

EXPERIMENTAL

Synthesis. All the starting materials were of analytical purity (A.R.) grade, and were obtained from commercial

---

[1] To whom correspondence should be addressed.

sources. NH$_4$VO$_3$ (1.11 g) was put into a Teflon-lined stainless steel autoclave with a capacity of 80 ml, and dissolved with distilled water ($\sim$60 ml) up to 75% capacity. An appropriate amount of hydrazine monohydrate (N$_2$H$_4 \cdot$H$_2$O) was added to this solution to give an 8.0% N$_2$H$_4$ aqueous solution. Immediately, a deep-colored solution formed due to the reduction of vanadium(VI). We then added NH$_3 \cdot$H$_2$O to control the pH value at $\sim$9.2. The autoclave was sealed and maintained at 170°C and autogenerated pressure for 15 days. The reaction solution was neither shaken nor stirred during the heating period. The resulting black precipitate was collected by filtering, washed with distilled water many times, and then dried in vacuum at 70°C for 5 hours. To investigate the effect of reaction conditions on the features of the final products, a series of experiments with various temperatures, heating durations, and concentrations of N$_2$H$_4$ were carried out.

Characterization of structure, composition, and morphology. X-ray powder diffraction analysis (XRD) was conducted out on a Rigaku D/Max X-ray diffractometer at a scanning rate of 0.05 degree per second with 2θ ranging from 5 to 65 degrees, using graphite monochromated CuK$_\alpha$ radiation ($\lambda = 1.5418$ Å). The PC programs Treor and Fullprof (the LeBail method) (21) were employed to solve the structure according to powder XRD data. A transmission electron microscope (TEM) operated at 200 kV was employed to characterize the morphology of the products. Images were collected in a bright field. Copper grids (300 mesh) coated with an amorphous carbon film were obtained commercially. Samples were prepared by placing drops of diluted ethanol with dispersed nanocrystallites on the surface of grids. At the same time, the electron diffraction pattern (ED) was recorded with typical crystallites observed. The compositions of the samples were determined by thermogravimetric analysis (TG) combined with X-ray energy dispersive spectroscopy (EDS). Infrared spectroscopy (IR) was recorded in a KBr matrix. Redox titration was conducted to determine the oxidation state of vanadium on the basis of the following method. First, a definite amount of as-prepared sample was dissolved quickly in 60 ml of 1.7 M H$_2$SO$_4$ solution operating under a N$_2$ atmosphere. The obtained solution was designated Sol(I). The concentration of standard KMnO$_4$ solution was determined by titrating with Na$_2$C$_2$O$_4$. The valence difference between the oxidation states of vanadium in the as-prepared sample and in completely oxidized V(VI) in VO$_2^+$ ions in the resulting solution could be determined by titrating Sol(I) with the standard KMnO$_4$ solution. With the addition of KMnO$_4$, the color of Sol(I) became yellow gradually. A sudden color change from light yellow to deep orange indicates the titration endpoint. In order to understand the evolution of phases upon heating, the as-prepared samples were subjected to differential scanning calorimetric analysis (DSC) in a flowing high-purity N$_2$ atmosphere in a temperature range from 30°C to 620°C.

RESULTS AND DISCUSSION

The sample of vanadium oxide hydrate obtained hydrothermally at 170°C for 15 days was characterized by XRD analysis. Its XRD pattern shown in Fig. 1a indicates its good phase purity, and is nearly identical to the simulated pattern shown in Fig. 1b obtained by using the LeBail method (using the PC program Fullprof) (21) in the space group $P222$. All the diffraction peaks could be indexed on the basis of orthorhombic symmetry. Simulation of the XRD pattern gave the lattice parameters $a = 6.015$, $b = 4.642$, and $c = 3.763$ Å. Other crystal symmetries, e.g., tetragonal and monoclinic systems, were also studied, but they did not lead to improved results, and have larger R_{wp} values than this orthorhombic unit cell. A TEM image for the sample obtained hydrothermally is shown in Fig. 2a. It indicates that the sample of VO$_2$ hydrate comprises needle-like nanocrystallites (7 nm $\times$ 35 nm). Figure 2b shows an electron diffraction pattern with the incident beam perpendicular to the needle-like crystallite axis. These spots sit well on the intercross sites of a rectangular network with the angle 90°. The corresponding d-spacing values were calculated for indexing the ED pattern. The observed (001) spot has a d value of 3.74 Å, close to the $c = 3.763$ Å from the LeBail simulation of the XRD pattern. The observed d-spacing of (120) planes is 2.18 Å, which is also in very good agreement with the d value of 2.17 Å calculated with the cell parameters $a = 6.015$ and $b = 4.642$ Å obtained from the
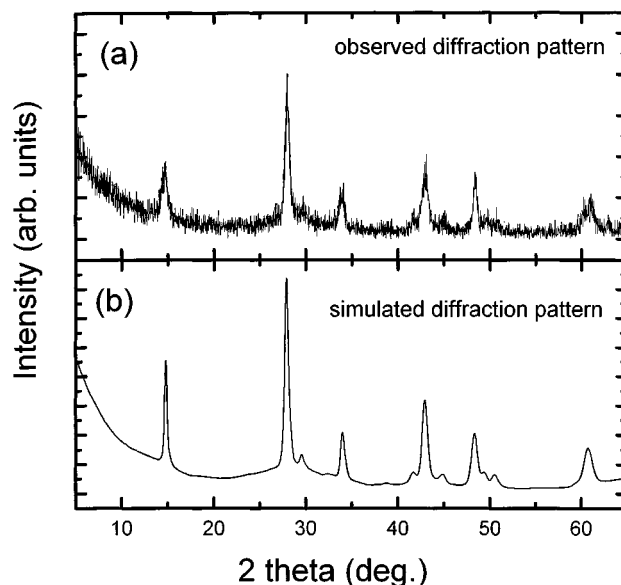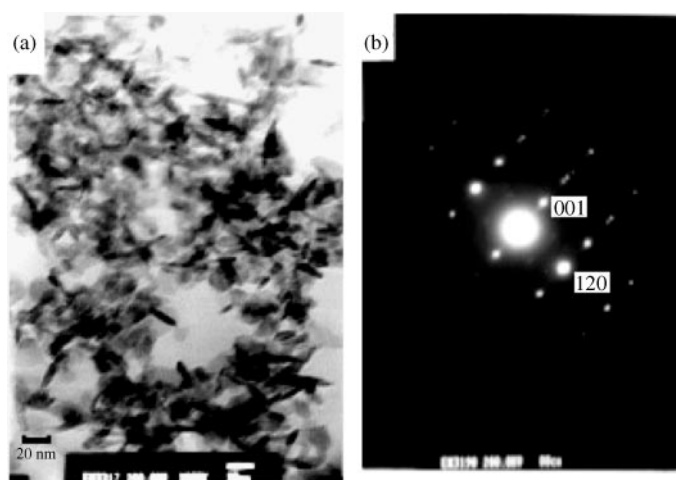

**FIG. 1.** Observed (a) and simulated (b) X-ray powder diffraction patterns for the sample of VO$_2 \cdot$H$_2$O obtained hydrothermally.

FIG. 2. (a) TEM image and (b) the corresponding electron diffraction pattern for the sample of $VO_2 \cdot H_2O$.

LeBail simulation of the XRD data. Therefore, the ED and XRD results are highly consistent and support the crystal symmetry as well as the calculated cell parameters. The (002) diffraction spot shows a weak "splitting" in the ED pattern, but the median point of the two "split" spots does not sit on the ideal (002) site; instead the relatively bright spot dwells well on this site. Thus, the observed "splitting" does not suggest the existence of a supperlattice and some kind of structural order. Actually, the as-prepared samples of vanadium oxide hydrates were found to be unstable under irradiation by an electron beam. So we attribute this "splitting" to a tiny structure change induced by the electron beam. Due to the great difficulty in preparing a highly crystallized sample of the title compound, the XRD data are not good enough to allow for Rietveld refinement.

The infrared spectrum for the sample obtained as shown in Fig. 3 indicates the existence of bound water and various V–O vibrations. The peak at $993 \, cm^{-1}$ was attributed to the stretching vibration $v(V=O)$ of the short-range order between vanadium and oxygen atoms. Another peak at $570 \, cm^{-1}$ showed the long-range stretching vibration $v(V-O-V)$. An evidence for the bound water is the strong broad absorbency peak around $3440 \, cm^{-1}$ corresponding to the stretching vibration $v(O-H)$ and a medium peak at $1633 \, cm^{-1}$ corresponding to the deformation vibrations $\delta(O-H)$ between oxygen and hydrogen atoms. TG analysis conducted in flowing N_2 atmosphere shows a weight loss of $\sim 15\%$ up to $400°C$, which is related to the procedure of dehydration. After the dehydrated sample was reheated in air for 12 hours, the resulting orange-colored solid was characterized as V_2O_5. According to the weight loss in dehydration and the weight increase in the following reheating, the chemical formula for the sample obtained hydrothermally can be determined as $VO_2 \cdot H_2O$. The valence

of vanadium in this sample was calculated to be $+4$ on the basis of the chemical formula. Redox titration was conducted to give a direct evidence for its oxidation state. According to the amount of $KMnO_4$ required for the titration, the difference between the oxidation state of V in the as-prepared sample and the $+5$ valence in the resulting VO_2^+ ions is 1.06. So the oxidation state of V in this sample is $+3.94$, very close to the theoretical value of $+4$. In addition, an EDS spectrum was recorded for the nanocrystallites of $VO_2 \cdot H_2O$. It indicates the existence of V and O (H cannot be detected this way) without any impurities such as elemental N.

In the experiment, we found that the formation of metastable $VO_2 \cdot H_2O$ strongly depends on the chemical reaction conditions: temperature, duration, and amount of reducing agent N_2H_4. The results of a series of experiments under various conditions are listed in Table 1. It reveals that the elevated temperature of $220°C$ favors the formation of thermodynamically stable rutile-type VO_2, and this novel metastable $VO_2 \cdot H_2O$ should be prepared at a temperature as low as $170°C$. The reaction duration must be controlled carefully to generate a single-phase $VO_2 \cdot H_2O$, because a well-developed crystalline $VO_2 \cdot H_2O$ must be produced over a long reaction time, while an exceedingly long duration leads to the conversion of metastable $VO_2 \cdot H_2O$ to rutile VO_2. The amount of reducing agent N_2H_4 also influences the final products remarkably. A low N_2H_4 concentration of 1.5% gives a poor-crystalline $VO_2 \cdot H_2O$ after 7 days, but it completely converts to rutile-type phase after 15 days. The high N_2H_4 concentration of 8.0% results in single-phase $VO_2 \cdot H_2O$ from 3 days to 15 days. Generally the longer the duration, the higher the crystallity of products obtained. The effects of much higher concentrations of N_2H_4 up to 65% were also investigated, but the resulting products did not differ from the previous samples. The
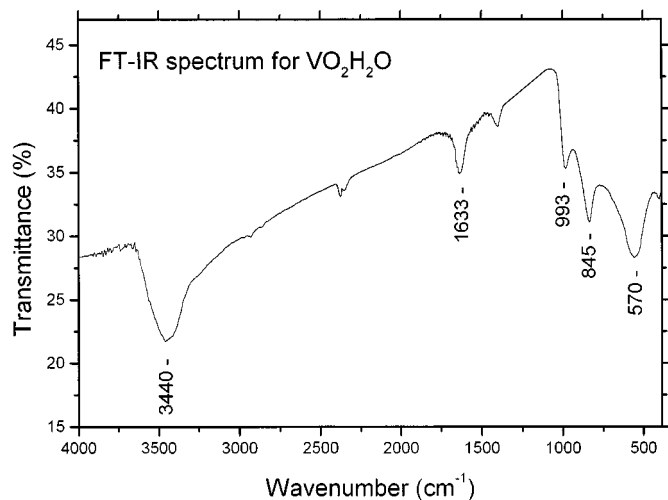
FIG. 3. Infrared spectrum of the sample of $VO_2 \cdot H_2O$.

TABLE 1
**Final Products of the Hydrothermal Reaction of NH$_4$VO$_3$ and N$_2$H$_4$ under Various Chemical Conditions**

Sample no.	Temp (°C)	Duration (days)	Concentration of N$_2$H$_4$ (%)	Final product obtained hydrothermally
1	170	7	8.0	Poor-crystalline VO$_2$·H$_2$O
2	170	15	8.0	Good-crystalline VO$_2$·H$_2$O
3	220	7	8.0	Rutile-type VO$_2$
4	220	15	8.0	Rutile-type VO$_2$
5	170	7	1.5	Poor-crystalline VO$_2$·H$_2$O
6	170	15	1.5	Rutile-type VO$_2$
7	170	15	65	Good-crystalline VO$_2$·H$_2$O

FIG. 4. TG and DSC curves for the sample of VO$_2$·H$_2$O beween 30 and 620°C.

optimum condition for preparing the novel VO$_2$·H$_2$O should be controlled at 170°C for 15 days with the starting N$_2$H$_4$ concentration of 8.0%.

The reducing agent N$_2$H$_4$ is used not only to generate a reducing atmosphere for the formation of reduced vanadium oxides, but perhaps also plays a key role in the control of the micromorphology. In our experiment, well-developed needle-like quasi-1-D nanocrystallites were prepared. A mechanism of molecular coordination and assembly via a vanadium–hydrazine complex as a building block can be suggested to explain the growth of the needle-like nanocrystallites, while other reducing agents, such as KBH$_4$ (17) and NH$_3$OHCl (22), give only amorphous or irregular poor-crystalline products. Due to the difficulty in *in situ* detection of an intermediate in a sealed autoclave, the reaction mechanism will be investigated further.

To understand the evolution of phases of VO$_2$·H$_2$O upon heating, the as-prepared samples were subjected to thermogavimetric analysis (TG) and differential scanning calorimetry (DSC) in a flowing N$_2$ atmosphere. The TG plot shown in Fig. 4a exhibits a weight loss of ∼15% corresponding to the loss of bound water. A portion of this sample was subjected to DSC; the recorded curve is shown in Fig. 4b. We see a very broad exothermic peak centered around 555°C. In order to understand the nature of the transformation associated with the DSC peak, we heated a portion of as-prepared VO$_2$·H$_2$O at various temperatures and examined the products by room-temperature X-ray powder diffraction. Figure 5a shows the diffraction pattern of the original sample VO$_2$·H$_2$O which was indexed on the basis of orthorhombic symmetry. The XRD pattern for the sample after heating in the temperature range from 300°C to 520°C for 24 hours shows the disappearance of the metastable phase VO$_2$·H$_2$O and the formation of (B)VO$_2$ and rutile-type VO$_2$ gradually. The two weak DSC peaks around 325°C and 375°C may correspond to the transformation to (B)VO$_2$ and rutile-type VO$_2$, respectively. But, because no sharp exotherm peaks were observed, these transformations may occur over a wide temperature range.
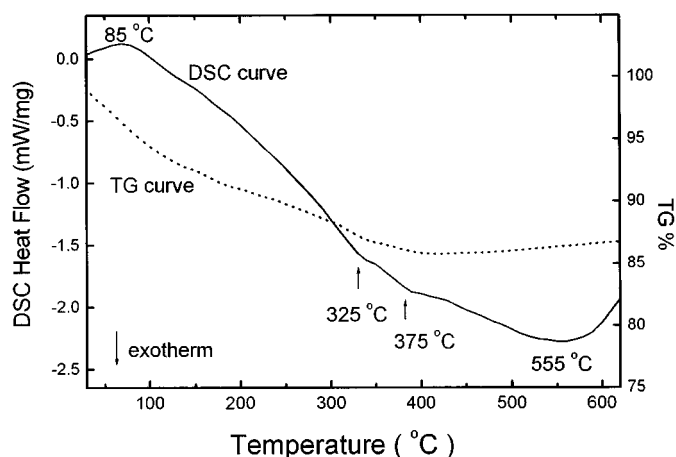
This phase transformation temperature is consistent with the previous report (17). Another portion of VO$_2$·H$_2$O was heated at an elevated temperature of 620°C; its XRD pattern shown in Fig. 5b reveals the existence of both (B)VO$_2$ and rutile-type VO$_2$ of higher crystallity. Previous literature (17) pointed out the transformation of (B)VO$_2$ to rutile-type VO$_2$ around 350°C, and a complete conversion around 500°C. However, the (B)VO$_2$ obtained by heating metastable VO$_2$·H$_2$O shows higher thermal stability and still appears up to 620°C. Additionally, a weak endothermic peak around 85°C may correspond to the loss and evaporation of bound water.
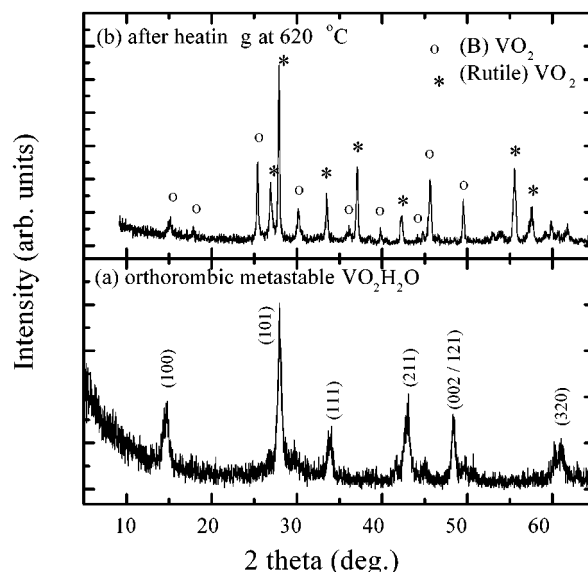
FIG. 5. X-ray diffraction pattern for the sample (a) obtained hydrothermally and (b) after heating VO$_2$·H$_2$O at 620°C for 24 hours in a high-purity N$_2$ atmosphere.

CONCLUSION

A long hydrothermal reaction of NH_4VO_3 and N_2H_4 generated needle-like nanocrystalline $VO_2 \cdot H_2O$ in a new orthorhombic metastable phase with lattice parameters $a = 6.015$, $b = 4.642$, and $c = 3.763$ Å, demonstrated by ED and XRD analysis. The formation of the $VO_2 \cdot H_2O$ phase strongly depends on the chemical reaction conditions of temperature, duration, and the amount of reducing agent N_2H_4. N_2H_4 could also be responsible for the control of the micromorphology of products. When the sample of $VO_2 \cdot H_2O$ is heated, it will transform to relatively more stable $(B)VO_2$ and rutile-type VO_2. Nanocrystalline transition metal oxides, such as VO_2, MnO_2, and their hydrates, were reported to show good performance as electrodes of high-energy density batteries (17). Herein, we prepared a new metastable phase of $VO_2 \cdot H_2O$ forming needle-like nanocrystallites that may find applications in the field of electrochemistry.

ACKNOWLEDGMENTS

REFERENCES

1. J. B. Goodenough and A. Hammett, "Landolt-Bernstein New Series Group III: Semiconductor," Vol. 17, Subvol. G, pp. 129–291, 1984.
2. J. Miki, Y. Osada, T. Konoshi, Y. Tachibana, and T. Shikada, *Appl. Catal. A* **137,** 93 (1996).
3. W. Li, J. R. Dahn, and D. S. Wainwright, *Science* **264,** 1115 (1994).
4. F. J. Morin, *Phys. Rev. Lett.* **3,** 34 (1959).
5. S. Minomura and H. Nagasaki, *J. Phys. Soc. Jpn.* **19,** 131 (1964).
6. R. E. Newnham and Y. M. De Haan, *Z. Kristallogr.* **117,** 235 (1962).
7. S. Asbrink, S. Friberg, A. Magneli, and G. Anderson, *Acta Chem. Scand.* **13,** 603 (1959).
8. J. Twu, C. Shih, T. Guo, and K. Chen, *J. Mater. Chem.* **7,** 2273 (1997).
9. H. Horiuchi, N. Morimoto, and M. Tokonami, *J. Solid State Chem.* **17,** 407 (1976).
10. E. A. Boylan, T. Chirayil, J. Hinz, P. Y. Zavalij, and M. S. Whittingham, *Solid State Ionics* **75,** 257 (1995).
11. G. Andersson, *Acta Chem. Scand.* **8,** 1599 (1954).
12. G. Andersson, *Acta Chem. Scand.* **10,** 623 (1956).
13. T. Metsuishi, *Jpn. J. Appl. Phys.* **6,** 1060 (1967).
14. F. Theobald, *J. Less-Common Met.* **53,** 55 (1977).
15. Y. Oka, T. Tao, and N. Yamamoto, *J. Solid State Chem.* **86,** 116 (1990).
16. F. Theobald, R. Cabala, and J. Bernald, *J. Solid State Chem.* **17,** 431 (1977).
17. C. Tsang and A. Manthiram, *J. Electrochem. Soc.* **144,** 520 (1997).
18. D. Hagrman, J. Zubieta, C. J. Warren, L. M. Meyer, M. J. Treacy, and R. C. Haushalter, *J. Solid State Chem.* **138,** 178 (1998).
19. S. A. Selim, Ch. A. Philip, and R. Ch. Mikhait, *Thermochim. Acta* **36,** 287 (1980).
20. C. L. Onnerud and J. O. Thomas, *J. Mater. Chem.* **5,** 1075 (1995).
21. "Fullprof" (J. Rodriguez-Carvajal, Ed.), Version 3.5d, Laboratoire Leon Brillouin, CEA-CNRS, Oct 1998.
22. V. Manivannan and J. B. Goodenough, *Mater. Res. Bull.* **33,** 1353 (1998).